Journal of Science: Advanced Materials and Devices 10 (2025) 100976

Contents lists available at ScienceDirect

Journal of Science: Advanced Materials and Devices

journal homepage: www.elsevier.com/locate/jsamd

Research Article

Sustainable composite from furfuryl alcohol and wood flour with outstanding fire resistance and its prediction using neural networks

Lukas Manas [a,b], Erika Pavlikova [a], Miroslav Mrlik [a], Roman Kolarik [a], Jozef Martinka [c], Peter Rantuch [c], Tomas Sedlacek [a], Tomas Plachy [a,*]

[a] Centre of Polymer Systems, University Institute, Tomas Bata University in Zlin, Trida Tomase Bati 5678, 760 01, Zlin, Czech Republic
[b] Faculty of Technology, Tomas Bata University in Zlin, Vavreckova 5669, 760 01, Zlin, Czech Republic
[c] Faculty of Materials Science and Technology in Trnava, Slovak University of Technology in Bratislava, Jána Bottu 2781/25, 917 24, Trnava, Slovakia

ARTICLE INFO

Keywords:
Cone calorimeter
Neural network prediction
Smoke production rate
Poly(furfuryl alcohol)
Green composites
Sustainable systems

ABSTRACT

Novel composites were successfully produced using renewable green sources, furfuryl alcohol resin, commonly obtained from biomass, and wood flour. Compared with a conventional melt-blending technique used for the preparation of wood-plastic composites, this unique approach, utilizing low-viscosity thermoset resin with high affinity for wood, enables the avoidance of excessive treatment of wood flour. Four flame retardants possessing different flame-retardant mechanisms (expandable graphite (EG), ammonium dihydrogen phosphate (ADP), Exolit OP560 and dimethyl propane phosphonate) at two loading levels (7.5 and 15 wt%) were used to suppress the flammability of the composites evaluated by a cone calorimeter test, limiting oxygen index and UL 94. All investigated flame retardants significantly reduced maximum value of heat release rate (HRR) (EG and ADP approx. up to 75 %) and, moreover, ADP and EG significantly reduced the total smoke production (EG up to 25 % and ADP up to 96 %) confirming outstanding and unusual flammability suppression considering HRR reduction and a decrease in smoke production rate (SPR) at the same time. Besides that, the neural network prediction models for HRR and SPR from test time and mass loss rate were created and trained, giving the possibility to predict HRR and SPR values from simple and cheap tests, providing only mass loss rate at specific conditions.

1. Introduction

Due to efforts to reduce the utilization of fossil sources and with pressure for sustainability, there are tendencies to find novel material compositions involving renewable sources. Wood flour (WF) is a cheap resource obtained from renewable wood waste and is often used in combination with thermoplastic polymers for the preparation of well-known wood-plastic composites (WPCs). Wood-plastic composites are thus materials combining a commonly thermoplastic polymer matrix with wood using melt blending and are utilized in many applications, such as terrace planks, various automotive components, pallets, furniture, *etc*. [1,2]. Commonly, WPCs enable overcoming drawbacks arising from the inherent nature of either plastic or wood materials, *e.g.,* wood absorption of moisture and degradation stability of polymeric materials. From an application point of view, however, important properties such as the flammability of the entire composite have to be suppressed using additive substances. Moreover, insufficient compatibility between thermoplastic resins and WF may lead to inferior performance of the composites.

Thermosetting systems may be used for large-wood parts impregnation to resist moisture and microbial decay, keep dimension stability [3], resist biological factors and for an aesthetic appearance [2,4]. For example, a furfurylation is a chemical modification of wood improving its application properties [5] by reducing its hygroscopicity [6], improving dimensional stability [7] and hardness, and enhance biodegradation [8]. Furfuryl alcohol (FA) is a low-viscosity liquid with high affinity for wood enabling its entrance to wood cells and chambers, where FA may be permanently fixed through polymerization to poly (furfuryl alcohol) (pFA) using a proper curing agent (*e.g.* maleic anhydride (MA)) [9,10]. Due to the sufficient compatibility of FA and wood, there is no need for additional treatment of used WF as in the case of WPCs prepared through a melt-blending process. Moreover, FA is prepared via hydrogenation of furfural, which may be obtained as a by-product from agricultural waste through biomass digestion and is therefore considered as a green and renewable source. In addition, MA was proven as a good compatibilizer for particulate filler and resin,

* Corresponding author.
E-mail address: plachy@utb.cz (T. Plachy).

https://doi.org/10.1016/j.jsamd.2025.100976
Received 19 April 2025; Received in revised form 19 August 2025; Accepted 21 August 2025
Available online 1 September 2025

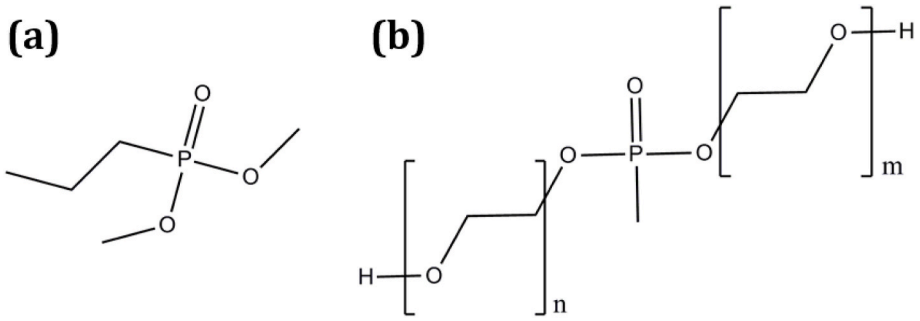

Fig. 1. Chemical structure of commercial fire retardants: (a) DMPP; and (b) Exolit OP560.

leading to an increase in the storage modulus of the composites [11].

Recently, thermoset systems have been used as a matrix and a binder in composites with WF, leading to superior WF-based composites (WFCs) when compared with WPCs prepared through melt blending. Xiao et al. [12] have introduced green WF-based thermosetting composites from castor-oil-based polyurethane containing up to 87.5 % of biomass, divided among 70 % of WF and 17.5 % of castor oil. This system exhibited enhanced interface compatibility and higher bending strength when compared with a similar WPC system based on polypropylene and WF prepared through a melt-blending method. Considering the internal structure, unlikely in WPCs, using adhesives may generally create chemical bonds and further physical cross-linking provides the compatibility leading to superior properties of the composite when compared to WPCs [12]. Mandal et al. [13] prepared WFCs using chemically modified epoxidized soybean oil, involving an excessive amount of chemicals and catalysts with an initiator. Similarly, the preparation of a green composite may be realized by utilizing conjugated linseed and soybean oil with a high content of wood fibers or WF (up to 85 %) [11]. Nabinejad et al. [14] have introduced a thermoset resin-based composite based on WF, oil palm shells and conventional unsaturated polyester, vinylester and epoxy resin produced from petrochemical resources. Distinguishing pre-treatments of WF showed a significant impact on the wettability of the WF by thermoset resin, leading to modification of the mechanical properties. To further increase of mechanical properties of prepared WFCs, additive manufacturing implementing 3D printing [15] has been applied. While a non-printed composite (a molded sample), utilizing WF and urea formaldehyde resin as a binder, showed flexural modulus and tensile strength of 5.4 GPa and 9.7 MPa, respectively, its 3D-printed analogue exhibited values of 6.8 GPa and 17 MPa. The increase in the mechanical properties can be explained by better densification of the system, leading to a significant decrease in void content in the sample [15]. Other bio-based systems utilized soy or wheat gluten protein to create outstanding wood adhesives for plywood preparation through a cross-linking reaction [16,17].

Wood flour composites are thus very promising systems that can be used in many applications and their properties may be further modified through particulate fillers [18] and, moreover, may be prepared from renewable sources. For systems based on conventional thermoset materials like epoxy resins or polyurethanes, many flame retardants with sufficient suppression of flammability have been developed and investigated. Besides well-known flame-retardant systems industrially implemented for thermosets, even flame retardants at research scale enhancing flame retardancy as well as mechanical and thermal behavior of the system based on variously modified polyhedral oligomeric silsequioxanes [19–23], barium phytate exhibiting synergistic effect with zinc oxide [24], organic sepiolite modified with coupling agent [25], and zinc borate together with aluminum diethyl phosphite [26] have been introduced. To evaluate the flammability of the composites, a cone calorimeter test, limiting oxygen index (LOI), and UL 94 test are commonly used [25,27]. To our best knowledge, however, in the case of WFCs based thermoset resins, information about their flammability is very limited, and there are only a few papers dealing with flammability. For example, excellent flammability suppression was tested by LOI and a cone calorimeter test of WFCs was achieved using sodium silicate and phytic acid [28]. On the other hand, Grzybek et al. [29] has tested various flame retardants for WFCs epoxidized with linseed oil, among which only clay with sodium silicate led to a reduction of heat release and smoke production at the same time.

In this study, the novel approach for the preparation of WFCs using renewable and green sources based on FA and WF is introduced, and their flammability is tested using flame retardants with various flame-retardant mechanisms. Furfuryl alcohol, commonly obtained from renewable biomass, was used as a thermoset matrix and a binder for WF. The goal was to evaluate the flammability of the composites implementing four different flame retardants (expandable graphite (EG), ammonium dihydrogen phosphate (ADP), Exolit OP560 and dimethyl propane phosphonate (DMPP)) and find the most suitable flame retardant considering their various retardant mechanism using a cone calorimeter test, LOI and UL 94 test. Upon heating, EG increases its volume [30] through an endothermic process and creates a foam layer and ADP thermally degrades to ammonia and phosphoric acid, which supports the creation of a charring layer on the burning wood surface [31,32]. Commercial flame retardants Exolit OP560 and DMPP are both liquid halogen-free phosphorus-based flame retardants (Fig. 1). Exolit OP 560 promotes char formation during combustion due to phosphorus content and hydroxyl groups, leading to a protective carbonaceous layer on the surface of a condensed phase. On the other hand, DMPP acts mainly in a gas phase, due to its decomposition to phosphorous molecules, inhibiting flame propagation through scavenging of radicals. Moreover, many research groups and institutes engaged in the investigation of material flammability do not have equipment for heat release rate (HRR) and smoke production rate (SPR) measurements due to their high acquisition costs. Therefore, the neural network models for HRR and SPR from test time and mass loss rate were created and trained in this study. Trained neural networks are available on request and can be used for HRR and SPR prediction from data that are obtained using relatively cheap and simple methods (test time and mass loss rate).

2. Experimental

2.1. Materials and chemicals

Furfuryl alcohol (purity 98 %, Sigma Aldrich, USA) and MA (purity 99 %. Acros Organics, USA) were used as delivered without any purification. As flame retardants, polyol with high content of phosphorus Exolit OP560 (Clariant, Switzerland), DMPP (Levagard, Lanxess, Germany), ADP (PENTA Chemicals, Czech Republic) and EG (AMG Graphite GK, Germany; carbon content >92 %, 80 % particles >150 μm) were used. Wood flour (type 15 E) was supplied by La.So.Le (Italy). The chemical structures of commercial products DMPP and Exolit OP560 are captured in Fig. 1.

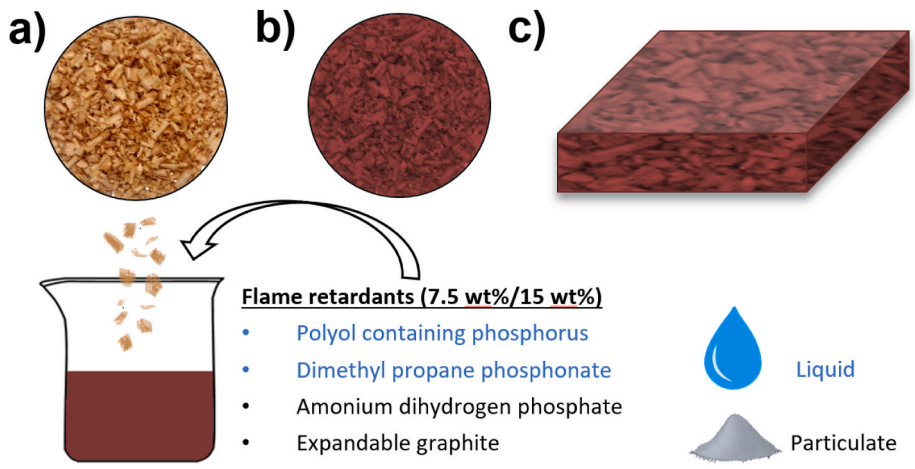

Fig. 2. A schematic illustration of preparation of wood-flour composite based on wood flour and furfuryl alcohol: a) various components used for production of the wood-flour composites - wood flour, furfuryl alcohol as a resin, maleic anhydride as a curing agent and various flame retardants (liquid or particulate flame retardants); b) saturated wood flour with furfuryl alcohol resin; c) the wood-flour composite prepared using a molding technique at 120 °C for 20 min.

Table 1
Composition of the prepared WFCs with various flame retardants (wt%).

Sample label	WF	FA	MA	DMPP	OP560	ADP[a]	EG
WFC	50	45	5	–	–	–	–
DMPP-7.5	50	38.25	4.25	7.5	–	–	–
DMPP-15	50	31.5	3.5	15	–	–	–
OP560–7.5	50	38.25	4.25	–	7.5	–	–
OP560-15	50	31.5	3.5	–	15	–	–
ADP-7.5	50	38.25	4.25	–	–	7.5	–
ADP-15	50	31.5	3.5	–	–	15	–
EG-7.5	50	38.25	4.25	–	–	–	7.5
EG-15	50	31.5	3.5	–	–	–	15

[a] The ADP was dissolved in demineralized water before its mixing with the thermoset system. Water content is not included due to presumption of its evaporation upon thermal treatment and chemical inertness regarding the used curing system.

2.2. Composite preparation

Firstly, MA was completely dissolved in FA in a weight ratio of 10:90 and the flame retardant was added. The mixture was homogenized using a glass stick and subsequently intensively mixed together with WF using a vacuum mixer (Twister venturi, Renfert, Germany) at 150 rpm for 10 min. The thoroughly mixed samples were then molded and cured at 120 °C for 20 min. A schematic illustration of the preparation process is captured in Fig. 2. In the case of samples with ADP, ADP was dissolved in a low amount of demineralized water before its addition into FA/MA solution. The flame retardants were used at two loading levels – 7.5 and 15 wt% of the total composite mass. The composition of the prepared samples is summarized in Table 1.

2.3. Composite characterization

A differential scanning analyzer (DSC; Mettler Toledo DSC1; Mettler Toledo; Switzerland) was used to characterize curing process of the prepared systems. Dynamic scans were performed with heating rate of 10 °C/min in a temperature range of 25–250 °C. In the case of isothermal scans, the sample was put into the furnace and immediately heated to an experiment temperature (no heating rate was set, the instrument reached the experiment temperature as fast as possible to avoid losing unnecessary curing heat). All the samples were loaded into an aluminum crucible closed with a lid with a pinhole on its top. A thermogravimetric analysis (TGA) was performed to observe thermal degradation of the prepared WFCs using a thermogravimetric analyzer (TGA Q500, TA Instruments, USA). The measurement ran at heating rate of 10 °C/min in a temperature range of 25–800 °C in an air atmosphere to simulate real conditions during combustion of the sample.

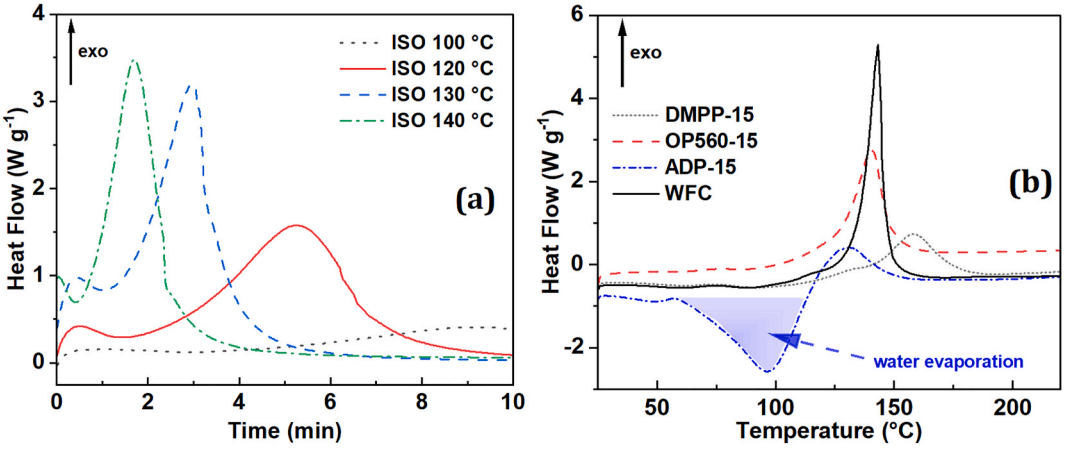

Fig. 3. DSC analysis of the prepared mixtures of FA/MA: (a) isothermal DSC scans of FA/MA (90:10 (w/w)) at various temperatures; (b) dynamic DSC scans for the systems with 15 wt% of flame retardants.

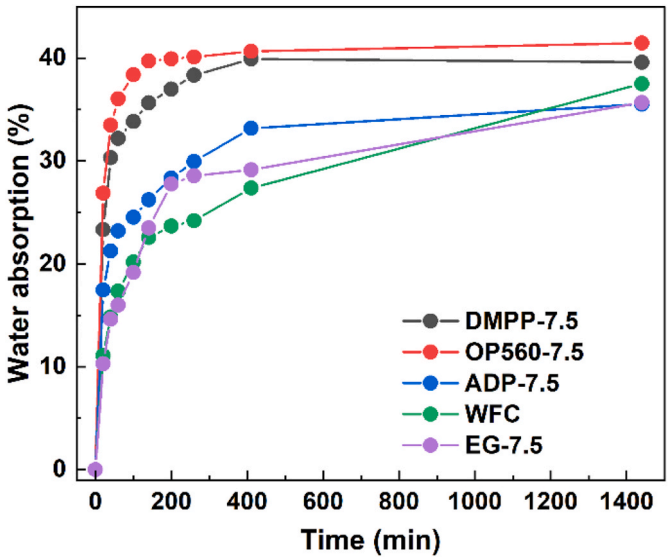

Fig. 4. Water absorption of prepared WFC with various flame retardants at loading level 7.5 %.

2.4. Water absorption test

Water absorption (WA) tests were performed using disk-shaped samples of approximately 20 mm and 3 mm in diameter and thickness, respectively. The specimens were immersed in 60 ml of distilled water at 23 °C and subsequently at certain time intervals, they were removed and weighed. Water absorption was calculated using the following equation (Eq. (1)) [33]:

$$WA\ (\%) = \frac{W_c - W_0}{W_0} \times 100 \quad (1)$$

where W_c is the weight of the specimen after immersion in the water and W_0 represents its original weight.

2.5. Fire hazard test

Fire hazard of investigated WFCs was evaluated based on key fire properties determined by the cone calorimeter quantifying (i) released heat as heat release rate (HRR), total heat release (THR), effective heat of combustion (EHC); (ii) released smoke as smoke production rate (SPR) and total smoke production (TSP); (iii) and mass loss as mass loss rate (MLR) and total mass loss (TML). Time to flashover was calculated from HRR according to Kokkala et al. [34] and C/VM2:2014 [35]. Both the cone calorimeter (Dual Cone Calorimeter, Fire Testing Technology, The United Kingdom) and measurement procedure were in accordance with ISO 5660–1:2015 standard [36]. The sample dimensions were

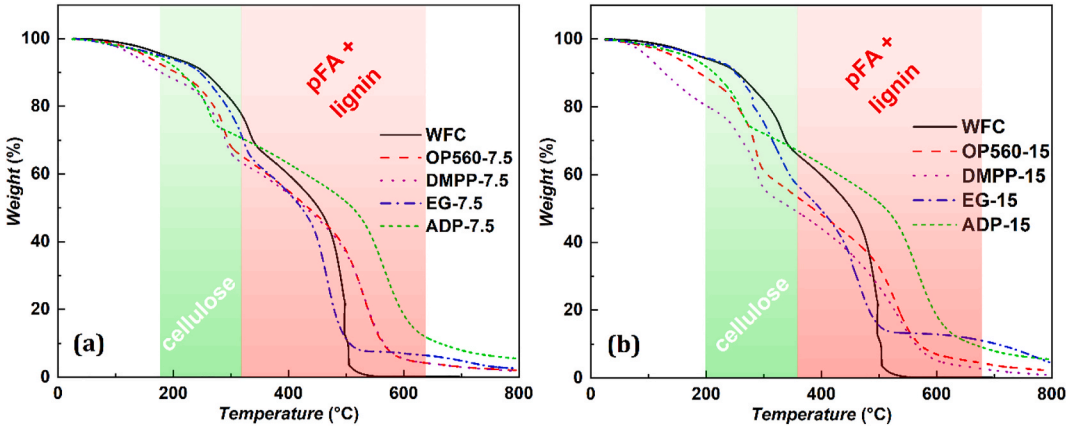

Fig. 5. Thermogravimetric analysis of prepared pFA WFC with various flame retardants at their concentration (a) 7.5 % and (b) 15 %. Measurements were performed in an air atmosphere.

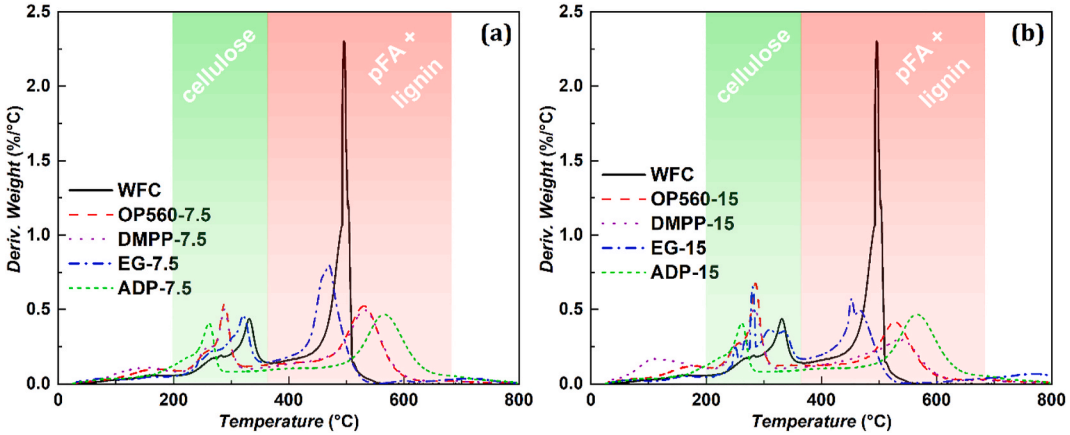

Fig. 6. A dependence of derivative weight loss obtained from thermogravimetric analysis of prepared pFA WFC with various flame retardants at their concentration (a) 7.5 % and (b) 15 %. Measurements were performed in an air atmosphere.

Table 2
Main fire characteristics of prepared pFA WFC with various content of flame retardants. The results of cone calorimeter test represent mean values of three independent measurements.

Properties	WFC	ADP-7.5	OP560–7.5	DMPP-7.5	EG 7.5
TTI (s)	18 ± 2	26 ± 1	17 ± 2	21 ± 5	20 ± 1
t_{FO} (min)	2 to 10	2 to 10	2 to 10	2 to 10	2 to 10
HRR_{max} (kW m^{-2})	675 ± 14	305 ± 9	591 ± 35	553 ± 17	182 ± 5
Time to HRR_{max} (s)	90 ± 5	63 ± 3	113 ± 3	95 ± 5	190 ± 10
MARHE (kW m^{-2})	330 ± 1	149 ± 2	285 ± 9	275 ± 9	136 ± 2
THR (MJ m^{-2})	95.2 ± 0.5	56.5 ± 0.2	106.5 ± 1.5	86.5 ± 0.5	76.0 ± 2.7
EHC (MJ kg^{-1})	22.87 ± 0.51	19.74 ± 0.95	22.73 ± 2.13	20.46 ± 0.51	19.63 ± 0.72
MLR_{max} (g m^{-2} s^{-1})	62.7 ± 1.9	51.0 ± 5.1	58.3 ± 3.3	54.6 ± 5.4	18.7 ± 2.2
Time to MLR_{max} (s)	80 ± 5	48 ± 3	98 ± 8	78 ± 3	108 ± 68
SPR_{max} (m^2 m^{-2} s^{-1})	9.19 ± 0.30	0.67 ± 0.46	8.65 ± 1.2	10.44 ± 0.47	2.15 ± 0.08
Time to SPR_{max} (s)	80 ± 5	30 ± 15	100 ± 5	80 ± 2	190 ± 10
TSP (m^2 m^{-2})	352.8 ± 2.7	12.4 ± 5.0	424.5 ± 20.5	515.6 ± 210.0	263.2 ± 12.8
LOI (%)	20.8	30.5	25.1	27.7	25.6
UL 94	–	V-0	V-0	V-0	–

Properties	ADP-15	OP560-15	DMPP-15	EG 15
TTI (s)	39 ± 23	17 ± 2	12 ± 1	30 ± 2
t_{FO} (min)	2 to 10	2 to 10	2 to 10	2 to 10
HRR_{max} (kW m^{-2})	185 ± 7	482 ± 23	476 ± 54	147 ± 9
Time to HRR_{max} (s)	83 ± 3	115 ± 5	113 ± 3	210 ± 5
MARHE (kW m^{-2})	98 ± 22	262 ± 12	282 ± 11	103 ± 4
THR (MJ m^{-2})	53.5 ± 4.5	91.6 ± 4.2	101.5 ± 1.8	68.7 ± 2.6
EHC (MJ kg^{-1})	16.09 ± 1.77	19.58 ± 0.11	22.01 ± 0.50	18.84 ± 0.37
MLR_{max} (g m^{-2} s^{-1})	37.6 ± 3.2	51.9 ± 1.6	47.5 ± 3.6	12.0 ± 0.1
Time to MLR_{max} (s)	78 ± 3	105 ± 5	100 ± 3	193 ± 3
SPR_{max} (m^2 m^{-2} s^{-1})	1.27 ± 0.05	6.59 ± 0.76	8.75 ± 0.56	1.07 ± 0.05
Time to SPR_{max} (s)	58 ± 28	108 ± 3	103 ± 3	168 ± 23
TSP (m^2 m^{-2})	43.6 ± 10.7	309.5 ± 27.0	538.5 ± 18.1	109.2 ± 3
LOI (%)	30.6	27.2	27.7	31.2
UL 94	V-0	V-0	V-0	V-0

TTI: time to ignition (s), t_{FO}: time to flashover (min), HRR_{max}: maximum value of heat release rate (kW m^{-2}), MARHE: maximum average rate of heat emission (kW m^{-2}), THR: total heat release (MJ m^{-2}), EHC: effective heat of combustion (MJ kg^{-1}), MLR_{max}: Maximum mass loss rate of per one square meter of sample (g m^{-2} s^{-1}), SPR_{max}: Maximum smoke production rate per one square meter of sample (m^2 m^{-2} s^{-1}), TSP: total smoke production per one square meter of sample (m^2 m^{-2}), sign ± denotes standard deviation.

(100x100x3)±0.5 mm (length x width x thickness) and the heat flux from a cone heater to the sample surface was 50 ± 0.5 kW m^{-2}. Measurement of each WFCs sample was repeated three times and average values together with standard deviations are presented as final results.

The four models of neural network prediction have been created in the MATLAB 2020b software (in the Neural Network Toolbox environment). The first model for prediction of HRR from MLR; the second model for prediction of SPR from MLR; the third model for prediction of SPR from HRR; and, finally, fourth model for prediction of SPR from both parameters MLR and HRR. The test time (in seconds) together with MLR (g m^{-2} s^{-1}) were used as an input in the first and second prediction model. The HRR (kW m^{-2}) or SPR (m^2 m^{-2} s^{-1}) were used as a desired output in the first or second prediction model, respectively. The test time together with HRR was used as the input and SPR was used as desired output in the third prediction model. Finally, test time together with MLR and HRR were used as the input and SPR was used as the desired output in the fourth model. The three-layer (input layer with two or three neurons, hidden layer with twenty neurons and an output layer with two neurons) feed-forward neural network was used. Sigmoid activation function for hidden neurons and linear activation function for input and output neurons were used. The Levenberg–Marquardt training algorithm was used. A total 3249 tuple values (3-tuple for the first to third model and 4-tuple for the fourth model) were used for training (2275 values), validation (487 values) and testing (487 values) of neural network models. For their testing, data used for the training or validation phase was excluded. Details regarding the structure and theory of the used neural network may be found for example in Martinka et al. [37] and Godovcin et al. [38].

The limiting oxygen index (LOI) was measured according to ISO 4589–2:2017 (under ambient temperature) [39]. Sample dimensions were: (150 × 7 × 3)±0.5 mm (length × width × thickness).

The flammability performance of WPC materials was evaluated according to the UL 94 – Standard for Safety of Flammability of Plastic Materials for Parts in Devices and Appliances. For the test, test specimens of dimensions 125 × 13 mm were prepared. Each specimen was suspended vertically, and a Bunsen burner flame was applied to the bottom edge for 10 s. If the flame was extinguished, after 15 s it was re-applied for another 10 s. A cotton indicator was placed below the sample in case of dripping particles.

3. Results and discussion

To determine the temperature for molding of the samples, curing reactions of pFA were investigated at isothermal conditions at temperatures of 100, 120, 130, and 140 °C. At 100 °C, the characteristic exothermic peak representing curing reaction was not observed (Fig. 3a) and a curve exhibited just a slight increase within 10 min indicating too low temperature for curing of the samples [40]. With increasing temperature of the experiment, the characteristic curing peak occurred confirming undergoing curing reaction; nevertheless, at temperature 140 °C and 130 °C the WF begin to degrade according to further investigations. Since it has been proved that higher temperature or longer curing time can lead to a denser cross-linked network, it can also initiate degradation of the WF filler leading to inferior properties of the composite [11]. Therefore, curing temperature 120 °C was found to be the most appropriate with a reasonable curing time and without noticeable degradation of the WF.

Utilizing dynamic heating scans (Fig. 3b), a curing reaction of pFA starts around 100 °C and 100 % degree of conversion is achieved slightly over 150 °C with the value of the total curing reaction enthalpy 345 J g^{-1}. Using flame retardants at the concentration of 15 wt% insignificantly affected the pFA curing reaction except for DMPP, which shifted the curing temperature to higher values. The DMPP did not participate in the curing reaction and its molecule reduced the concentration of FA/MA in the system and created possible steric barrier hindering proper curing process. Therefore, the curing process of such a system is much slower than in the case of others flame retardants. Unlikely DMPP, Exolit OP560 can be possibly involved in the curing reaction of pFA due to presence of hydroxyl groups. The system with Exolit OP560 exhibited the curing peak at the same position as pFA but with a lower value of the total enthalpy of curing 287 J g^{-1}. On the contrary, ADP solution significantly reduced the total enthalpy, however, in this case, the result is skewed because part of the exothermic reaction overlaps an endothermic area related to water evaporation. Nevertheless, it can be concluded that the flame retardants OP560 and ADP only slightly affect the curing reaction from the processing point of view. On the other hand, the flame retardant DMPP shifted the curing process to higher temperatures.

One of the most important characteristics of composites containing the wood is their WA characteristic. Generally, not only concentration but as well size of the wood particles considerably affects WA. Smaller

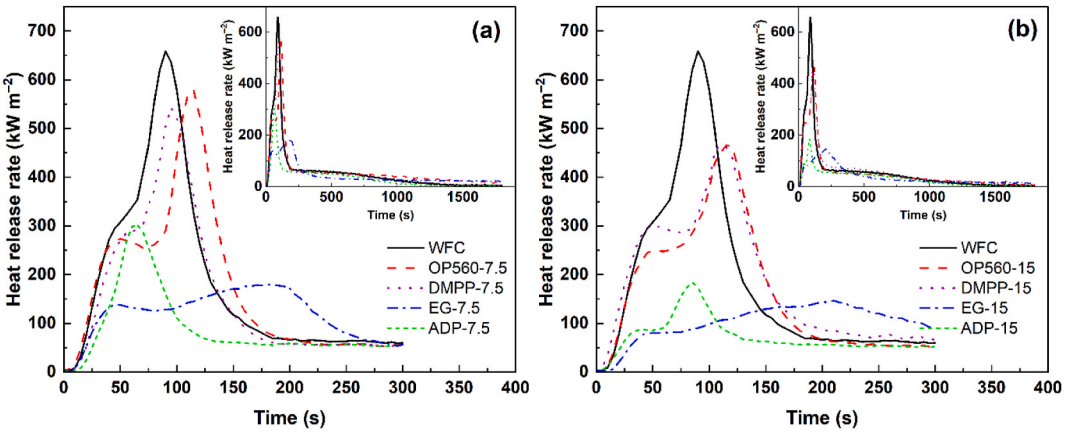

Fig. 7. Heat release rate of pFA WFC with various flame retardants at two concentration levels: (a) 7.5 wt% and (b) 15 wt%. The inset represents the full-length HRR for entire duration of the measurement.

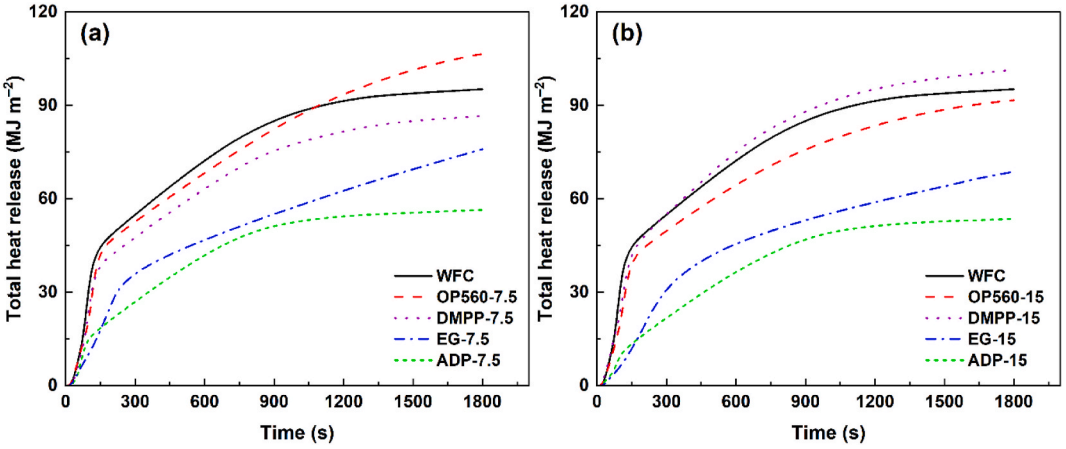

Fig. 8. Total heat release of pFA WFC with various flame retardants at two concentration levels: (a) 7.5 wt% and (b) 15 wt%.

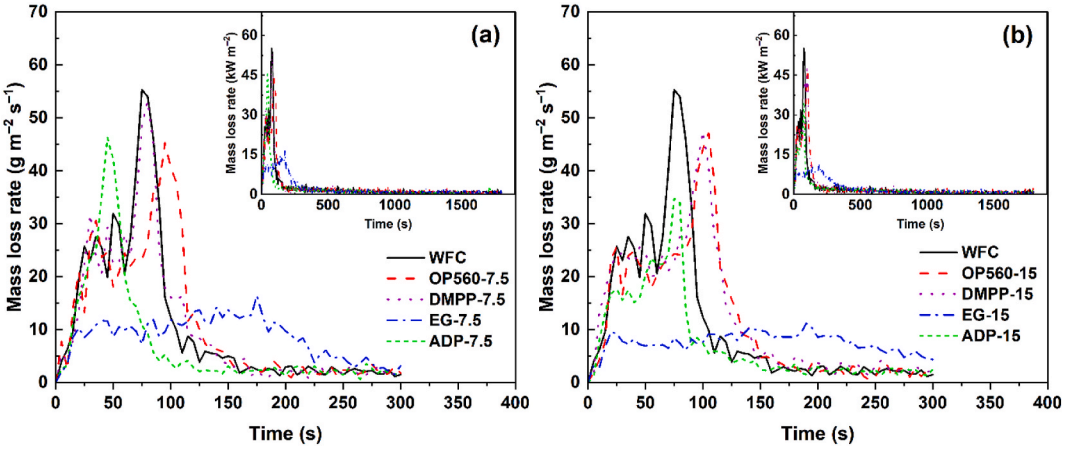

Fig. 9. Mass loss release rate of pFA WFC with various flame retardants at two concentration levels: (a) 7.5 wt% and (b) 15 wt%.

particles fill the voids in the interface area between WF and the surrounding pFA matrix eliminating the moisture flow paths [41].

Among all tested samples the highest WA value after 24 h was found for OP560–7.5 (41.5 %) and DMPP-7.5 (39.6 %). DMPP is a volatile low molecular weight substance unable to react with pFA and may be possibly washed from the material or migrate to its surface consequently promoting water absorption. In the case of sample OP560–7.5 a similar phenomenon can be expected, even though the Exolit OP560 may partially participate in the curing reaction due to presence of hydroxyl groups. On the other hand, samples ADP-7.5 and EG-7.5 exhibited even lower WA when compared with pure WFC sample. While EG, as the particulate flame retardant could possibly repulse the water molecules and act as a steric barrier to hinder absorption of water molecules, to the sample ADP-7.5 a define amount of water was added before molding

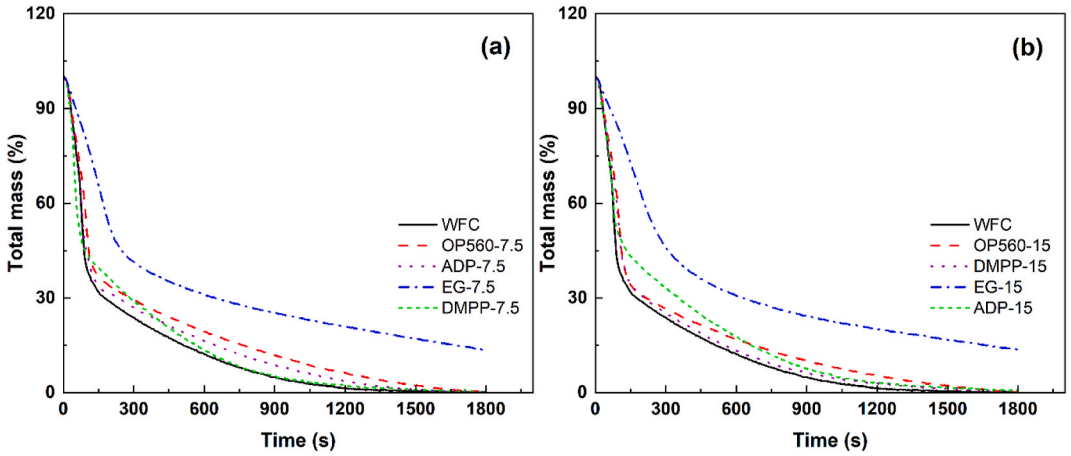

Fig. 10. Total mass of pFA WFC with various flame retardants at two concentration levels: (a) 7.5 wt% and (b) 15 wt%.

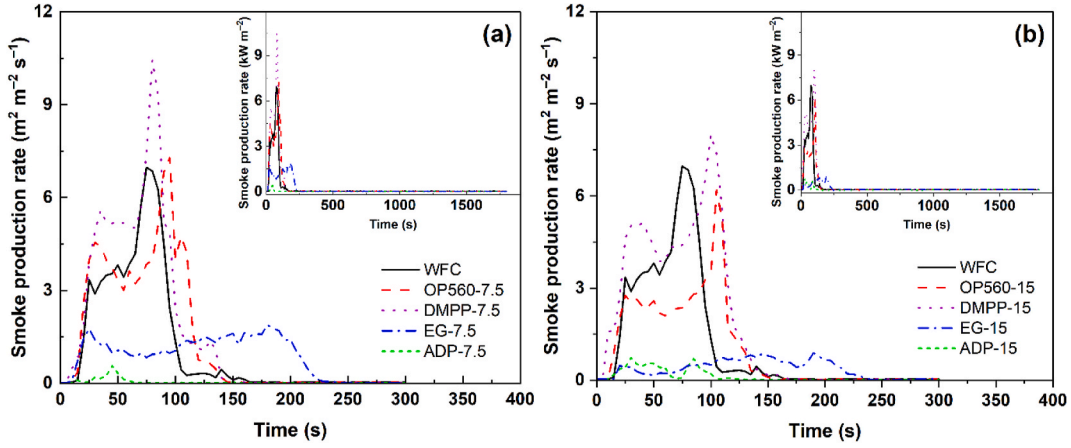

Fig. 11. Smoke production rates from pFA WFC with various flame retardants at two concentration levels: (a) 7.5 wt% and (b) 15 wt%.

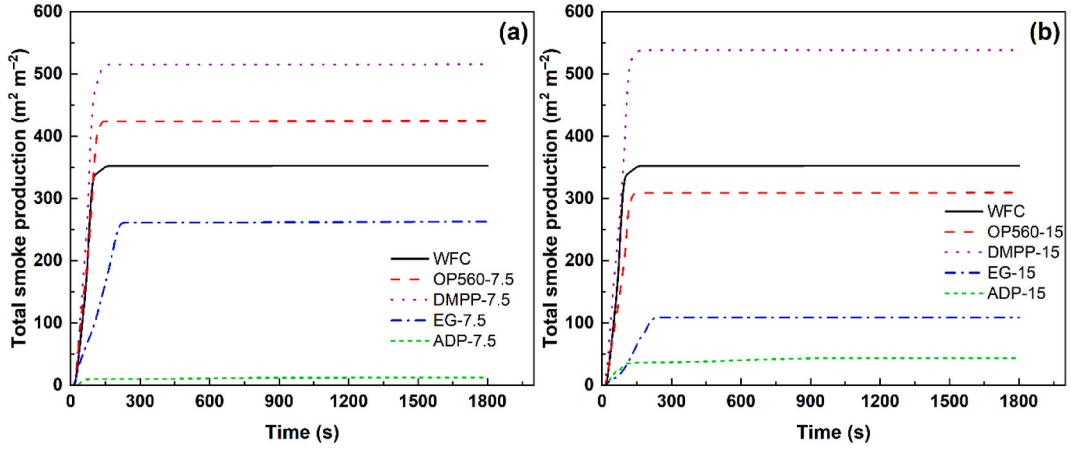

Fig. 12. Total smoke production rate from pFA WFC with various flame retardants at two concentration levels: (a) 7.5 wt% and (b) 15 wt%.

that could possibly lead to solidification of the composite and thus enhancing its barrier properties (Fig. 4).

Thermogravimetric analysis was performed in an air atmosphere in order to simulate real conditions during combustion of the material. The weight loss dependence of the samples on the temperature exhibited 3 main areas (Fig. 5a and b). The first area up to 200 °C represents degradation of low molecular and volatile fractions together with moisture, whose amount can be possibly significantly higher for the samples with flame retardants due to their lower consistency when compared with reference WFC. In the second area from approximately 200 °C up to 375 °C, hemicellulose and cellulose of WF is decomposed together with the flame retardants into char residues and low molecular compounds (CO_2, CO, CH_4 H_2O *etc.*) [42,43]. Interestingly, the thermal stability of the cellulose of WF is better for the reference sample without

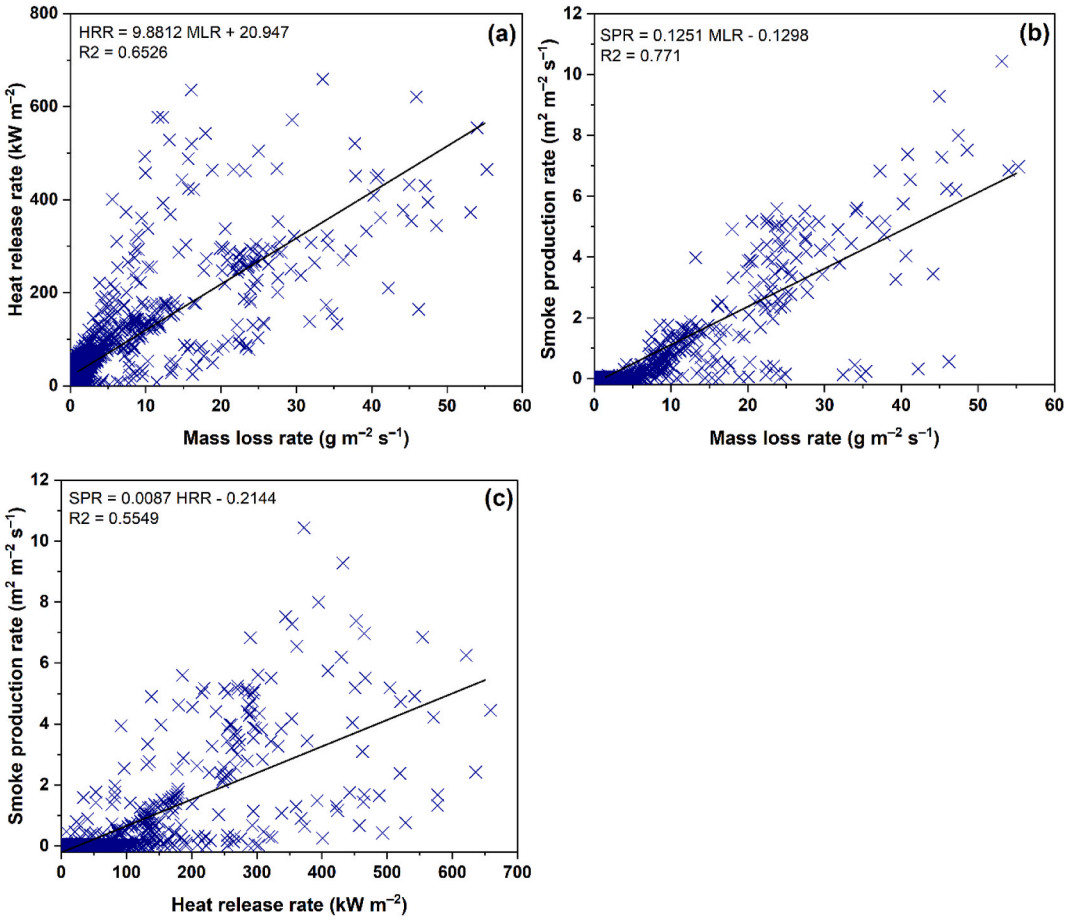

Fig. 13. Dependencies of (a) HRR on MLR, (b) SPR on MLR and (c) SPR on HRR for investigated WFC.

addition of flame retardants (Fig. 6a and b). The peak of derivative weight, which represents the highest rate of decomposition, is shifted about 50 °C to lower temperatures for the samples containing flame retardants. On the other hand, the third drop in the weight over 375 °C represents mainly decomposition of pFA [44] and lignin, as the part of wood with the highest thermal stability due to aromatic character into basic molecular compounds as in the case of cellulose [45]. The peak of derivative weight of this drop is shifted to higher temperatures when compared with reference sample [42,46]. When compared with cellulose, due to aromatic structure of lignin during its decomposition significantly higher amount of char is produced (carbon residues) [45] that can be even promoted in the presence of flame retardants containing phosphor and phosphonic acid explaining the shift of the peak [31].

The main fire characteristics of investigated WFCs are shown in Table 2. Investigated flame retardants improved fire characteristics of WFCs (an increase in time to ignition and simultaneously a decrease in all other parameters in Table 2) in almost all cases. This behavior is unique, because most flame retardants usually improve only one group of properties (*e.g.* HRR and derived parameters), while other properties (*e.g.* smoke production) get worse. The behavior of typical (today common and known flame retardants) is described in Papaspyrides and Kiliaris [47] and Arao and Visakh [48]. Flame retardants exhibiting flame spread rate reduction and smoke suppression at the same time have been investigated and described in detail by Chen et al. [49] and Jiao et al. [50]. Flame retardants described in the cited scientific works have been developed and designed for synthetic polymers and plastics, however, in the case of wood and wood composites there are only few reports, where the flame retardants have both effects [29,31]. Obtained results (Table 2) proved that investigated flame retardants have significant both effects (flame and smoke suppression) and have potential to further fill this gap. The ADP and EG flame retardants seem to be very effective from this point of view, whereas OP560 and DMPP improved only parameters tied with HRR. It has been shown before that some liquid phosphor-containing flame retardants have only limited effect on flame reduction in pure furan resin [51].

Time to flashover in the range of 2–10 min (Table 2) categorizes all examined samples to Group Number 2 materials according to C/VM2:2014 (flashover is reached later than 2 min, but before 10 min) [35]. Therefore, investigated flame retardants have virtually no effect on the flashover category according to C/VM2:2014 [35].

The sharp increase of HRR from the moment of ignition followed by a rapid decline (as a consequence of sample burn out) was observed for most samples (Fig. 7). WFCs samples treated by both EG and ADP shown different behavior (gradual growth and slow decline of HRR). Besides that, both EG and ADP showed significantly lower values of THR than untreated WFC reference samples (Fig. 8) due to formation of a solid charred layer on the surface of WFCs. Effect of EG and ADP as support for the formation of a carbon layer is generally known (EG during fire conditions increases volume and create foam layer, while ADP thermally degrade to ammonia and phosphoric acid). Phosphoric acid supports creation of charring layer on the burning wood surface. The composition and properties of the remaining carbon layer (created from wood and wood-based composites treated by ADP and/or EG were studied in some scientific works, *e.g.* Refs. [31,32]. The charred layer protects the sample from the flame and creates an insulating and compact layer providing thermal isolation and suppressing transition of gases and volatile substances from/into the sample [52,53]. Thus, more components remain in the condensed phase in a form of char, and amount of volatile and toxic substances penetrating through the meso-phase serving as a fuel for the

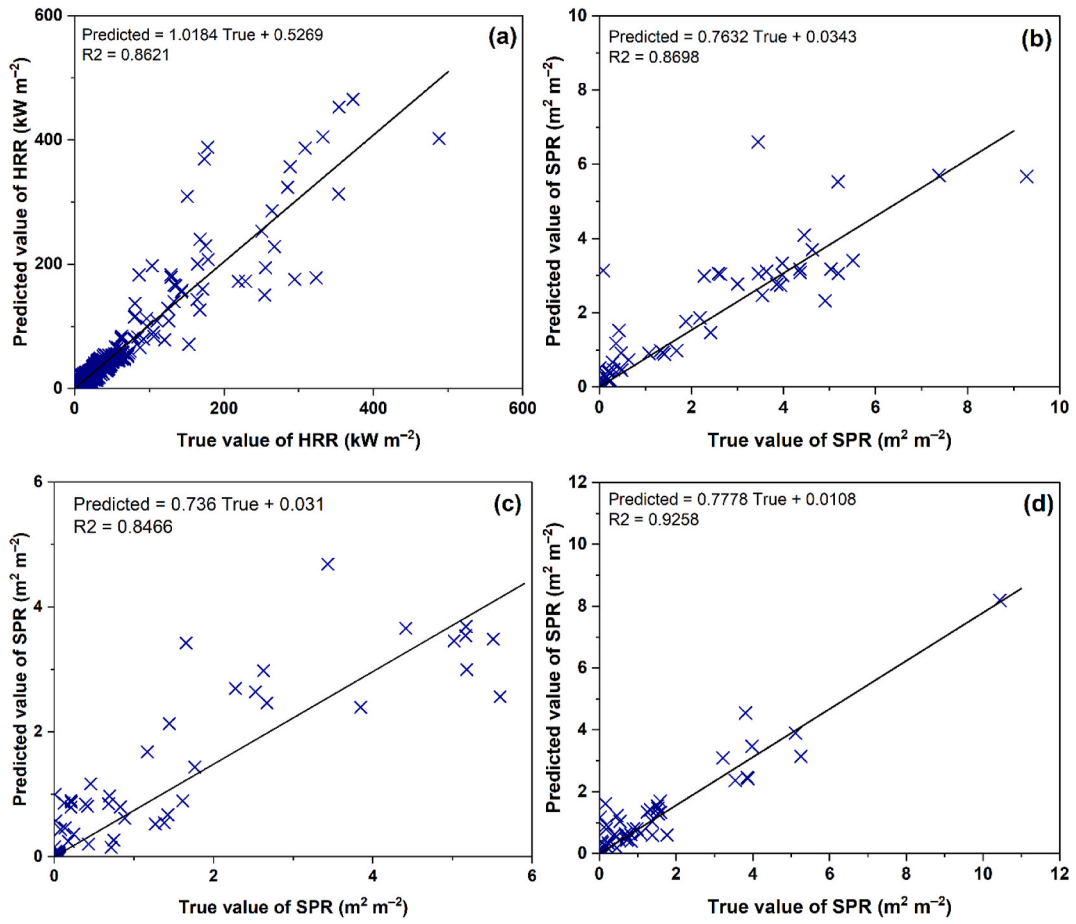

Fig. 14. Regression of values predicted by the trained neural networks vs. true value during the testing phase for (a) prediction of HRR from MLR, (b) prediction of SPR from MLR, (c) prediction of SPR from HRR, and (d) prediction of SPR from both MLR and HRR.

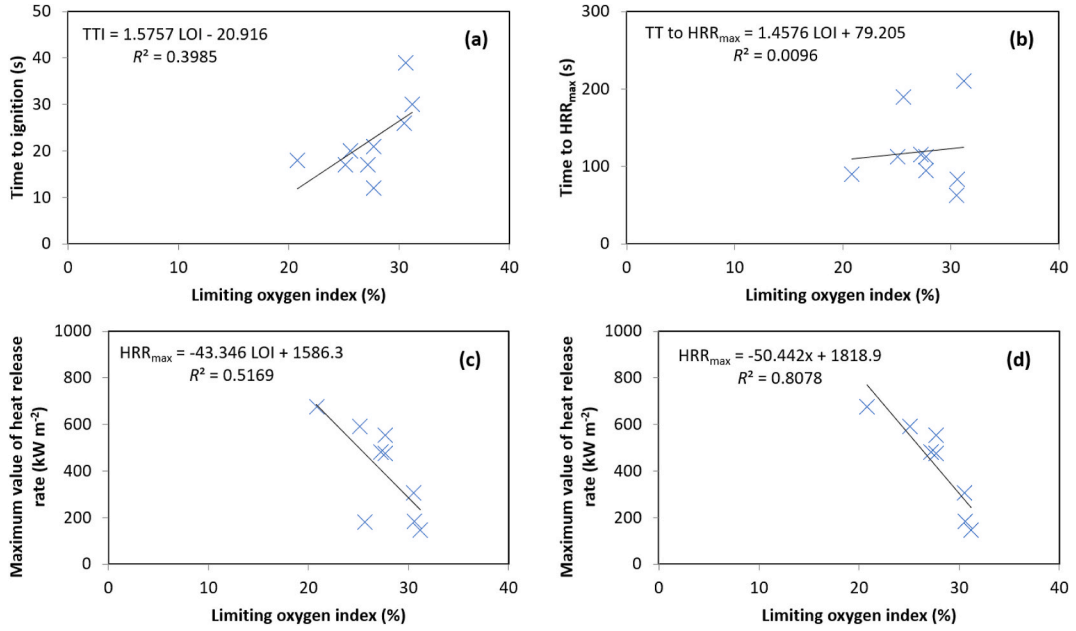

Fig. 15. Correlation of limiting oxygen index (LOI) and (a) time to ignition (TTI), (b) time to HRR_{max} (TT to HRRmax), (c) HRR_{max}, and (d) HRR_{max} after discarding one extreme value.

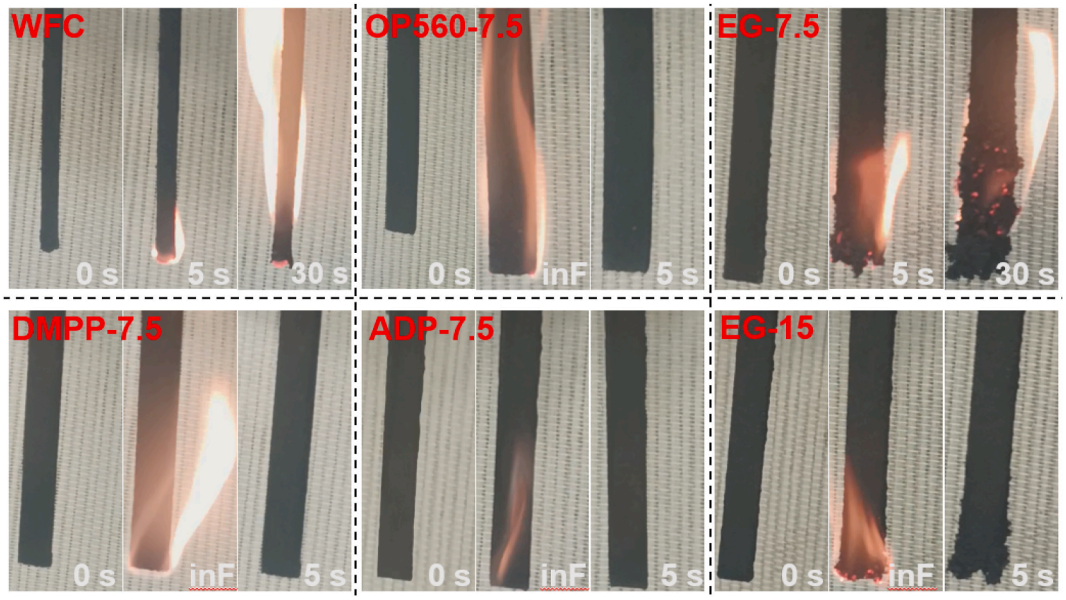

Fig. 16. Images of the samples under investigation during UL 94 test: (0 s) – sample before the test; (5 s) – sample 5 s after removal of the source of flame; (30 s) – sample 30 s after removal of fire; (inF) – sample just before removal of the fire (exposure to fire 2 × 10 s).

fire significantly decreases [20]. For flame retardants Exolit OP560 and DMPP, which are liquid halogen-free phosphorus-based flame retardants similar curve trends were found. Under combustion of material these flame retardants decompose to phosphorous radicals quenching with hydrogen and hydroxyl radicals in a gas phase [25,27]. Moreover, Exolit OP5650 may also promote isolative char layer formation due to higher amount of hydroxyl groups slightly shifting the position of the $HRR_{max.}$

The shapes of HRR curves (Fig. 7) corresponded well with MLR curves (Fig. 9). Besides that, the course of THR (Fig. 8) and inverse course of total mass (Fig. 10) are almost the same. The reason is fact, that HRR as well as THR are determined only by MLR of the sample and its effective heat of combustion (EHC) [54]. Thus, in addition to MLR, EHC is one of the most important fire parameters. Average EHC of wood and wood-based products according to Gunther et al. [55] is 17.72 ± 0.87 MJ kg^{-1}, which is lower than EHC found for reference WFC (Table 2). This may be caused by higher water content in samples investigated by Gunther et al. [55] and simultaneously presence of pFA acting as the binder in WFCs investigated in this study.

Smoke production rate of pFA WFCs with various flame retardants is shown in Fig. 11 and TSP of the same samples during the cone calorimeter test is shown in Fig. 12. The course of SPR (Fig. 11) and TSP (Fig. 12) is very similar to HRR (Fig. 7) and THR (Fig. 8). Noticeably, there is an obvious significant impact of ADP at both concentration levels and EG at 15 wt% concentration on smoke reduction. The values of SPR and TSP for the reference sample WFC and WFCs treated with Exolit OP650 and DMPP are approximately (in the same order of a magnitude) the same as values for other organic polymers presented by Sonnier et al. [56,57]. However, values of SPR and TSP of ADP and EG-15 are significantly lower than data presented by Sonnier et al. [56, 57] confirming their very high efficiency for smoke reduction.

As mentioned above, the curves of MLR, HRR and SPR on the one hand, and THR, total mass and TSP have very similar course (Figs. 7–12). The mutual dependencies (regression) of MLR, HRR and SPR are shown in Fig. 13. Especially dependence of SPR on MLR is relatively strong (R^2 is almost 0.80). From scientific papers of Sonnier et al. [56,57] it is obvious that the dependence of SPR on HRR corresponds with burning phase (ignition, flame combustion and flameless combustion). Consequently, the neural networks models for prediction of HRR and SPR from MLR considering the test time (the test time is associated with burning phase) have been designed and trained in this study. Results (regression of predicted vs. true values) for test data are shown in Fig. 13. Test data was used neither for training nor for validation. Thus, Fig. 13 describes well-trained neural network model accuracy. The accuracy for prediction of HRR or SPR from MLR (Fig. 14a–c) is sufficient for large amount of application. Accuracy for SPR prediction form MLR and HRR (Fig. 14d) is excellent. This model can be used for very accurate SPR and TSP measurements by the cone calorimeter, while laser or gravimetric system for smoke measure is not needed. Designed and trained neural networks are available upon request.

Limiting oxygen index expresses to some extent the resistance of a material to ignition. Comparison of LOI with time to ignition, HRR_{max} and time to HRR_{max} indicate some correlation of LOI with these parameters (Fig. 15). Fig. 15d shows relatively strong mutual correlation of LOI and HRR_{max} after discarding one extreme value. Comparison of obtained LOI values with values published in other scientific works [58] indicate that investigated flame retardants show similar LOI values than other recent flame retardants used for wood and wood based products. Specifically wood based products protected by flame retardant based on guanidine phosphate−zinc borate have LOI value in the interval from 22.4 to 47.8 % [58].

UL 94 is a common test for plastic materials giving fast comparison of flammability among prepared specimens. While the reference sample WFC did not reach any rating according to UL 94 since the sample completely burnt, except the sample EG-7.5 all tested samples at both concentrations level reached rating V-0 (Table 2, Fig. 16). Even though during the combustion of the sample EG-7.5 expansion of EG occurred (Fig. 16), unlikely during the cone calorimeter test, the created carbon layer was not sufficient when the sample was exposed directly to a source of flame. However, even though the sample EG-7.5 completely burnt, the flame spread was significantly slower than in the case of WFC. In the case of other samples reaching rating V-0 after removal of the source of flame, the flame extinguished in few seconds (Fig. 16). For the other flame retardants than EG, only behavior of the samples with lower concentration is shown.

4. Conclusion

The impact of four flame retardants of (i) expandable graphite, (ii)

ammonium dihydrogen phosphate, (iii) polyol with high content of phosphor Exolit OP560 and (iv) dimethyl propane phosphonate at two loading levels (7.5 and 15 wt%) on the thermal stability (investigated by the thermogravimetric method) and on the fire hazard of novel fully green wood flour composites has been investigated in this study. The btained results proved a unique impact of two investigated flame retardants (ammonium dihydrogen phosphate and expandable graphite) on the flammability of the prepared wood flour-based composites. These two flame retardants significantly improved practically all fire characteristics and also thermal stability of the prepared composites (significantly reduced maximum values of heat release rate, total heat release, smoke production rate and total smoke production). All flame retardants further reduced the flammability of the composites tested by limiting the oxygen index test and UL 94.

Besides that, the neural network prediction models for the prediction of both heat release rate and smoke production rate from test time and mass loss rate were created and trained. The coefficient of determination (R^2) for these prediction models was in the interval from 0.85 to 0.93, confirming the eligibility of these for heat release rate and smoke production rate prediction. The obtained results may be very useful for material design for a large number of applications where the flammability of materials plays a crucial role, such as materials for outside constructions or basic furniture.

CRediT authorship contribution statement

Lukas Manas: Investigation. **Erika Pavlikova:** Writing – original draft, Methodology, Investigation, Formal analysis. **Miroslav Mrlik:** Methodology, Conceptualization. **Roman Kolarik:** Investigation. **Jozef Martinka:** Writing – original draft, Validation, Data curation, Conceptualization. **Peter Rantuch:** Methodology, Investigation, Formal analysis. **Tomas Sedlacek:** Writing – review & editing. **Tomas Plachy:** Writing – review & editing, Writing – original draft, Validation, Methodology, Investigation, Conceptualization.

Declaration of competing interest

The authors declare the following financial interests/personal relationships which may be considered as potential competing interests: Nothing to declare. If there are other authors, they declare that they have no known competing financial interests or personal relationships that could have appeared to influence the work reported in this paper.

Acknowledgments

This work was supported by the Ministry of Education, Youth and Sports of the Czech Republic – DKRVO (RP/CPS/2024–28/003). This work was supported by the Slovak Research and Development Agency under the contract No. APVV-24-0143. This work was also supported by the Scientific Grant Agency of the Ministry of Education, Research, Development and Youth of the Slovak Republic and the Slovak Academy of Sciences (project No. VEGA 1/0755/25).

References

[1] G.J. Guo, V.L. Finkenstadt, Y. Nimmagadda, Mechanical properties and water absorption behavior of injection-molded wood fiber/carbon fiber high-density polyethylene hybrid composites, Adv. Compos. Hybrid Mater. 2 (2019) 690–700, https://doi.org/10.1007/s42114-019-00116-5.

[2] M. Ramesh, L. Rajeshkumar, G. Sasikala, D. Balaji, A. Saravanakumar, V. Bhuvaneswari, R. Bhoopathi, A critical review on wood-based polymer composites: processing, properties, and prospects, Polymers 14 (2022), https://doi.org/10.3390/polym14030589.

[3] M.H. Liu, F. Guo, H.K. Wang, W.T. Ren, M.D. Cao, Y. Yu, Highly stable wood material with low resin consumption via vapor phase furfurylation in cell walls, ACS Sustain. Chem. Eng. 8 (2020) 13924–13933, https://doi.org/10.1021/acssuschemeng.0c03172.

[4] K. Xu, G. Du, S. Wang, Wood Plastic Composites: Their Properties and Applications, 2021.

[5] D. Sandberg, A. Kutnar, G. Mantanis, Wood modification technologies - a review, iFor. Biogeosci. For. 10 (2017) 895–908, https://doi.org/10.3832/ifor2380-010.

[6] T.T. Yang, K.R. Zhang, C.T. Mei, E.N. Ma, J.Z. Cao, Effects of furfurylation on interactions between moisture sorption and humidity conditioning of wood, Wood Sci. Technol. 56 (2022) 703–720, https://doi.org/10.1007/s00226-022-01375-0.

[7] M.H. Liu, S.Y. Lyu, L.M. Peng, L.P. Cai, Z.H. Huang, J.X. Lyu, Improvement of toughness and mechanical properties of furfurylated wood by biosourced epoxidized soybean oil, ACS Sustain. Chem. Eng. 9 (2021) 8142–8155, https://doi.org/10.1021/acssuschemeng.1c01358.

[8] Y.M. Dong, K.L. Wang, J.Z. Li, S.F. Zhang, S.Q. Shi, Environmentally benign wood modifications: a review, ACS Sustain. Chem. Eng. 8 (2020) 3532–3540, https://doi.org/10.1021/acssuschemeng.0c00342.

[9] L.Z. Kong, H. Guan, X.Q. Wang, In situ polymerization of furfuryl alcohol with ammonium dihydrogen phosphate in poplar wood for improved dimensional stability and flame retardancy, ACS Sustain. Chem. Eng. 6 (2018) 3349–3357, https://doi.org/10.1021/acssuschemeng.7b03518.

[10] W.J. Li, D. Ren, X.X. Zhang, H.K. Wang, Y. Yu, The furfurylation of wood: a nanomechanical study of modified wood cells, Bioresources 11 (2016) 3614–3625.

[11] R.L. Quirino, J. Woodford, R.C. Larock, Soybean and linseed oil-based composites reinforced with wood flour and wood fibers, J. Appl. Polym. Sci. 124 (2012) 1520–1528, https://doi.org/10.1002/app.35161.

[12] F. Xiao, F.Q. Weng, D.Y. Guo, E. Koranteng, H.B. Zhou, Q.X. Wu, Preparation and characterization of thermosetting wood flour composite material with high biomass content, Polym. Compos. 42 (2021) 4822–4830, https://doi.org/10.1002/pc.26192.

[13] M. Mandal, P. Begum, R.C. Deka, T.K. Maji, Wood flour thermoset composites using chemically modified epoxidized soybean oil, Eur. J. Wood Wood Prod. 77 (2019) 569–580, https://doi.org/10.1007/s00107-019-01396-w.

[14] O. Nabinejad, D. Sujan, M.E. Rahman, I.J. Davies, Effect of filler load on the curing behavior and mechanical and thermal performance of wood flour filled thermoset composites, J. Clean. Prod. 164 (2017) 1145–1156, https://doi.org/10.1016/j.jclepro.2017.07.036.

[15] K. Pitt, O. Lopez-Botello, A.D. Lafferty, I. Todd, K. Mumtaz, Investigation into the material properties of wooden composite structures with in-situ fibre reinforcement using additive manufacturing, Compos. Sci. Technol. 138 (2017) 32–39, https://doi.org/10.1016/j.compscitech.2016.11.008.

[16] X.T. Zhao, T. Liu, R.X. Ou, X.L. Hao, Q. Fan, C.G. Guo, L.C. Sun, Z.Z. Liu, Q. W. Wang, Fully biobased soy protein adhesives with integrated high-strength, waterproof, mildew-resistant, and flame-retardant properties, ACS Sustain. Chem. Eng. 10 (2022) 6675–6686, https://doi.org/10.1021/acssuschemeng.2c00742.

[17] X.Y. Chen, Z.Y. Yang, F.X. Yang, J. Zhang, A. Pizzi, H. Essawy, G.B. Du, X.J. Zhou, Development of easy-handled, formaldehyde-free, high-bonding performance biosourced wood adhesives by co-reaction of furfuryl alcohol and wheat gluten protein, Chem. Eng. J. 462 (2023), https://doi.org/10.1016/j.cej.2023.142161.

[18] A. Hazarika, T.K. Maji, Strain sensing behavior and dynamic mechanical properties of carbon nanotubes/nanoclay reinforced wood polymer nanocomposite, Chem. Eng. J. 247 (2014) 33–41, https://doi.org/10.1016/j.cej.2014.02.069.

[19] X.M. Ye, X.Y. Jing, Y.L. Liu, Z.Q. Han, F. Yang, L. Qiao, J. Ren, L.G. Meng, Z.M. Li, W.S. Wang, J. Li, Y.C. Li, Simultaneously flame retarding and toughening of epoxy resin composites based on two-dimensional polyhedral oligomeric silsesquioxane/polyoxometalate supramolecular nanocrystals with ultralow loading, ACS Appl. Mater. Interfaces 16 (2024) 49763–49777, https://doi.org/10.1021/acsami.4c09639.

[20] Y.L. Liu, X.M. Ye, F. Yang, T. Liu, Y. Wang, Z.M. Li, F. Xiao, W.S. Wang, J. Li, Y. C. Li, Construction of flame-retarded epoxy resin composites based on two-dimensional disc-shaped Janus supramolecular nanosheets, Polym. Degrad. Stabil. 229 (2024), https://doi.org/10.1016/j.polymdegradstab.2024.110934.

[21] X.M. Ye, Y. Feng, P.P. Tian, Z.M. Li, Y.C. Li, W.S. Wang, J. Li, L. Qiao, K. Wang, W. C. Zhang, Y.T. Pan, R.J. Yang, Engineering two nitrogen-containing polyhedral oligomeric silsesquioxanes (N-POSSs) to enhance the fire safety of epoxy resin endowed with superior thermal stability, Polym. Degrad. Stabil. 200 (2022), https://doi.org/10.1016/j.polymdegradstab.2022.109946.

[22] X.M. Ye, Y.F. Zhang, Q.R. Guo, F. Yang, Y.L. Liu, J.K. Bai, T. Liu, X.Y. Jing, F. Xiao, F.C. Li, W.S. Wang, J. Li, Y.C. Li, Designing silicon-containing nanotube architectures to impart epoxy resin high-efficient flame retardancy, Polym. Degrad. Stabil. 232 (2025), https://doi.org/10.1016/j.polymdegradstab.2024.111129.

[23] X.M. Ye, Z.Q. Han, P.P. Tian, T. Liu, X.N. Meng, C.K. Yuan, W.S. Wang, Y.C. Li, Copper-containing tetra-phenyl polyhedral oligomeric silsesquioxane endows epoxy resin with reinforcements in the thermal stability, flame retardancy and smoke suppression, Compos. Commun. 37 (2023) 6, https://doi.org/10.1016/j.coco.2022.101459.

[24] X. Zhang, X.X. Qu, Q.H. Guan, R.Z. Li, Z. Wang, H. Xie, Rigid polyurethane foam with improved thermal stability and flame retardancy modified by barium phytate and zinc oxide, Case Stud. Therm. Eng. 72 (2025) 18, https://doi.org/10.1016/j.csite.2025.106261.

[25] X. Zhang, Q.H. Guan, S. Ding, Z. Wang, H. Xie, Improved thermal stability, flame retardancy and mechanical properties of casein-based rigid polyurethane foam modified with organic sepiolite, Constr. Build. Mater. 479 (2025) 16, https://doi.org/10.1016/j.conbuildmat.2025.141517.

[26] X. Zhang, S. Ding, Q.H. Guan, Z. Wang, H. Xie, Enhancing thermal properties, flame retardant and mechanical of multifunctional rigid polyurethane foam modified with zinc borate and aluminum diethyl hypophosphite, Appl. Therm. Eng. 278 (2025) 12, https://doi.org/10.1016/j.applthermaleng.2025.127427.

[27] X. Zhang, Z.Q. Wang, S. Ding, Z. Wang, X. Xie, Improved thermal insulation, mechanical properties, energy absorption and flame retardancy of bio-based rigid

polyurethane foam modified with calcium hydroxystannate, Constr. Build. Mater. 456 (2024) 21, https://doi.org/10.1016/j.conbuildmat.2024.139251.
[28] C.F. Lin, C. Zhang, O. Karlsson, J. Martinka, G.I. Mantanis, P. Rantuch, D. Jones, D. Sandberg, Phytic acid-silica system for imparting fire retardancy in wood composites, Forests 14 (2023), https://doi.org/10.3390/f14051021.
[29] J. Grzybek, M. Nazari, M. Jebrane, N. Terziev, A. Petutschnigg, T. Schnabel, Enhancing fire safety and thermal performance: wood composites with bio-based phase change materials and fire retardants for building applications, Fire Mater. 48 (2024) 838–846, https://doi.org/10.1002/fam.3238.
[30] T. Plachy, E. Pavlikova, R. Moucka, M. Cvek, Facile transformation of graphite composites into their porous analogues with superior electrical, thermal, and EMI shielding properties, Compos. Pt. B-Eng. 306 (2025) 8, https://doi.org/10.1016/j.compositesb.2025.112827.
[31] C.G. Guo, L. Zhou, J.X. Lv, Effects of expandable graphite and modified ammonium polyphosphate on the flame-retardant and mechanical properties of wood flour-polypropylene composites, Polym. Polym. Compos. 21 (2013) 449–456, https://doi.org/10.1177/096739111302100706.
[32] Y.C. Wang, G. Tang, J.P. Zhao, Y. Han, Effect of flaky graphite with different particle sizes on flame resistance of intumescent flame retardant coating, Results Mater. 5 (2020), https://doi.org/10.1016/j.rinma.2020.100061.
[33] A.M. Radzi, S.M. Sapuan, M. Jawaid, M.R. Mansor, Water absorption, thickness swelling and thermal properties of roselle/sugar palm fibre reinforced thermoplastic polyurethane hybrid composites, J. Mater. Res. Technol. 8 (2019) 3988–3994, https://doi.org/10.1016/j.jmrt.2019.07.007.
[34] M.A. Kokkala, P.H. Thomas, B. Karlsson, Rate of heat release and ignitability indices for surface linings, Fire Mater. 17 (1993) 209–216, https://doi.org/10.1002/fam.810170503.
[35] The Ministry of Business, Innovation and Employment, C/VM2, Verification Method: Framework for Fire Safety Design, first ed., 2014. Wellington, New Zealand, 2014.
[36] International Organization for Standardization, ISO 5660-1:2015. Reaction to Fire Tests - Heat Release, Smoke Production and Mass Loss Rate - Part 1: Heat Release Rate (Cone Calorimeter Method) and Smoke Production Rate (Dynamic Measurement), 2015.
[37] J. Martinka, P. Rantuch, F. Martinka, I. Wachter, T. Stefko, Improvement of heat release rate measurement from woods based on their combustion products temperature rise, Processes 11 (2023), https://doi.org/10.3390/pr11041206.
[38] P. Godovcin, J. Martinka, P. Rantuch, M. Hladova, J. Kopunek, M. Otajovicova, M. Z. Bendarikova, Impact of temperature and ultraviolet radiation on changes of colour of fir and spruce wood, Wood Res. 67 (2022) 894–907, https://doi.org/10.37763/wr.1336-4561/67.6.894907.
[39] International Organization for Standardization, ISO 4589-2:2017. Plastics — determination of burning behaviour by oxygen index. Part 2: Ambient-Temperature Test, 2017.
[40] N. Herold, T. Dietrich, W.J. Grigsby, R.A. Franich, A. Winkler, B. Buchelt, A. Pfriem, Effect of maleic anhydride content and ethanol dilution on the polymerization of furfuryl alcohol in wood veneer studied by differential scanning calorimetry, Bioresources 8 (2013) 1064–1075, https://doi.org/10.15376/biores.8.1.1064-1075.
[41] S.N. Kartal, S. Aysal, E. Terzi, N. Yilgor, T. Yoshimura, K. Tsunoda, Wood and bamboo-PP composites: fungal and termite resistance, water absorption, and FT-IR analyses, Bioresources 8 (2013) 1222–1244, https://doi.org/10.15376/biores.8.1.1222-1244.
[42] D. Xing, J. Li, Effects of heat treatment on thermal decomposition and combustion performance of larix spp. wood, Bioresources 9 (2014) 4274–4287, https://doi.org/10.15376/biores.9.3.4274-4287.
[43] M. Becidan, O. Skreiberg, J.E. Hustad, Products distribution and gas release in pyrolysis of thermally thick biomass residues samples, J. Anal. Appl. Pyrolysis 78 (2007) 207–213, https://doi.org/10.1016/j.jaap.2006.07.002.
[44] N. Guigo, A. Mija, R. Zavaglia, L. Vincent, N. Sbirrazzuoli, New insights on the thermal degradation pathways of neat poly(furfuryl alcohol) and poly(furfuryl alcohol)/SiO_2 hybrid materials, Polym. Degrad. Stabil. 94 (2009) 908–913, https://doi.org/10.1016/j.polymdegradstab.2009.03.008.
[45] E.A. Varol, Ü. Mutlu, TGA-FTIR analysis of biomass samples based on the thermal decomposition behavior of hemicellulose, cellulose, and lignin, Energies 16 (2023) 19, https://doi.org/10.3390/en16093674.
[46] W. Hoareau, W.G. Trindade, B. Siegmund, A. Castellan, E. Frollini, Sugar cane bagasse and curaua lignins oxidized by chlorine dioxide and reacted with furfuryl alcohol: characterization and stability, Polym. Degrad. Stabil. 86 (2004) 567–576, https://doi.org/10.1016/j.polymdegradstab.2004.07.005.
[47] C.D. Papaspyrides, P. Kiliaris, Polymer Green Flame Retardants, Elsevier, 2014.
[48] P.M.Y.A. Visakh, Flame Retardants, Springer, 2015.
[49] X.L. Chen, L. Liu, C.M. Jiao, Y. Qian, S.X. Li, Influence of ferrite yellow on combustion and smoke suppression properties in intumescent flame-retardant epoxy composites, High Perform. Polym. 27 (2015) 412–425, https://doi.org/10.1177/0954008314553644.
[50] C.M. Jiao, X.L. Zhao, W.K. Song, X.L. Chen, Synergistic flame retardant and smoke suppression effects of ferrous powder with ammonium polyphosphate in thermoplastic polyurethane composites, J. Therm. Anal. Calorim. 120 (2015) 1173–1181, https://doi.org/10.1007/s10973-014-4377-z.
[51] B.K. Kandola, W. Pornwannachai, J.R. Ebdon, Flame retardance of a bio-based furan resin: effects of added flame retardants, Polym. Degrad. Stabil. 220 (2024), https://doi.org/10.1016/j.polymdegradstab.2023.110637.
[52] L.Z. Yang, Y.P. Zhou, W. Wang, Z.F. Guo, Predicting charring rate of woods exposed to time-increasing and constant heat fluxes, J. Anal. Appl. Pyrolysis 81 (2008) 1–6, https://doi.org/10.1016/j.jaap.2007.06.006.
[53] N. Fischer, S. Treml, Charring rate of wood and derived timber products in relation to density, particle size and arrangement of the particles, Eur. J. Wood Wood Prod. 70 (2012) 327–335, https://doi.org/10.1007/s00107-011-0565-8.
[54] M.J. Hurley, D. Gottuk, J.R. Hall, K. Harada, E. Kuligowski, M. Puchlovsky, J. Torero, J.M. Watts, C. Wieczorek, SFPE Handbook of Fire Protection Engineering, Springer, New York, NY, 2016.
[55] B. Gunther, K. Gebauer, R. Barkowski, M. Rosenthal, C.T. Bues, Calorific value of selected wood species and wood products, Eur. J. Wood Wood Prod. 70 (2012) 755–757, https://doi.org/10.1007/s00107-012-0613-z.
[56] R. Sonnier, L. Dumazert, M. Vangrevelynghe, C. Brendle, L. Ferry, Intrinsic smoke properties and prediction of smoke production in national bureau of standards (NBS) smoke chamber, Fire 6 (2023), https://doi.org/10.3390/fire6030109.
[57] R. Sonnier, H. Vahabi, C. Chivas-Joly, New insights into the investigation of smoke production using a cone calorimeter, Fire Technol. 55 (2019) 853–873, https://doi.org/10.1007/s10694-018-0806-z.
[58] L.Y. Wang, Y.B. Yang, H.B. Deng, W.Y. Duan, J.J. Zhu, Y. Wei, W. Li, Flame retardant properties of a guanidine phosphate-zinc borate composite flame retardant on wood, ACS Omega 6 (2021) 11015–11024, https://doi.org/10.1021/acsomega.1c00882.